Published in final edited form as:
Neuron. 2010 November 4; 68(3): 428–441. doi:10.1016/j.neuron.2010.10.020.

Transsynaptic progression of amyloid-β-induced neuronal dysfunction within the entorhinal-hippocampal network

Julie A. Harris[1,2], **Nino Devidze**[1], **Laure Verret**[1,2], **Kaitlyn Ho**[1], **Brian Halabisky**[1,2], **Myo T. Thwin**[1], **Daniel Kim**[1], **Patricia Hamto**[1], **Iris Lo**[1], **Gui-Qiu Yu**[1], **Jorge J. Palop**[1,2], **Eliezer Masliah**[3,4], and **Lennart Mucke**[1,2,*]

[1] Gladstone Institute of Neurological Disease, San Francisco, CA 94158, USA

[2] Department of Neurology, University of California, San Francisco, CA 94158, USA

[3] Departments of Neurosciences, University of California, San Diego, San Diego, CA 92093, USA

[4] Department of Pathology, University of California, San Diego, San Diego, CA 92093, USA

SUMMARY

The entorhinal cortex (EC) is one of the earliest affected and most vulnerable brain regions in Alzheimer's disease (AD), which is associated with amyloid-β (Aβ) accumulation in many brain areas. We show selective overexpression of mutant amyloid precursor protein (APP) predominantly in layer II/III neurons of the EC causes cognitive and behavioral abnormalities characteristic of mouse models with widespread neuronal APP overexpression, including hyperactivity, disinhibition, and spatial learning and memory deficits. Overexpression of APP/Aβ in the EC elicited abnormalities in synaptic functions and activity-related molecules in the dentate gyrus and CA1, as well as epileptiform activity in parietal cortex. Soluble Aβ was observed in the dentate gyrus and Aβ deposits in the hippocampus were localized to perforant pathway terminal fields. Thus, APP/Aβ expression in EC neurons can cause transsynaptic deficits, which could initiate the cortical-hippocampal network dysfunction observed in mouse models and human patients with AD.

INTRODUCTION

Alzheimer's disease (AD) is characterized by progressive memory impairments (Blennow et al., 2006). Since the encoding of various forms of memory requires an intact entorhinal-hippocampal circuit (Squire et al., 2004; Eichenbaum and Lipton, 2008), it is not surprising that this network is severely affected by AD. Neurons in the superficial layers of the entorhinal cortex (EC) form synapses via the perforant pathway in all hippocampal subregions, including the dentate gyrus (DG), CA3, CA1, and subiculum, with the largest projection to the granule cells of the DG (van Groen et al., 2003; van Strien et al., 2009). In mice, DG granule cells receive afferent input primarily from layer II neurons of the EC; projections to CA3 and CA1 originate mostly from layer III (van Groen et al., 2003; van Strien et al., 2009). Synaptic connections between the mossy fibers of DG granule cells and CA3 neurons, and the Schaffer collaterals from CA3 to CA1 neurons complete the forward hippocampal polysynaptic circuit.

Within the entorhinal-hippocampal network, the EC is a particularly early target in AD. Significant loss of neurons in EC layer II occurs in beginning stages of AD (Gomez-Isla et

*Correspondence: lmucke@gladstone.ucsf.edu.

al., 1996). Neurofibrillary tangles (NFTs), a pathological hallmark of AD, are observed primarily in the EC in mild AD and then "spread" to the hippocampus and other cortical areas as the disease progresses (Braak and Braak, 1991; Braak et al., 2006). Structural and functional imaging studies also demonstrate early, selective atrophy and hypometabolism in the EC of patients with mild cognitive impairment or early-stage AD (Masdeu et al., 2005; Wu and Small, 2006).

Much evidence suggests that Aβ peptides, generated from amyloid precursor protein (APP) by proteolytic cleavage, play a causal role in AD pathogenesis (Walsh and Selkoe, 2004; Tanzi and Bertram, 2005). Although the precise mechanisms of Aβ toxicity are unclear, oligomeric forms of Aβ appear to alter the structure and function of synapses, which likely contributes to cognitive decline (Selkoe, 2008; Shankar et al., 2008; Palop and Mucke, 2009). Transgenic mouse models that overexpress mutant APP and produce high levels of Aβ recapitulate many features of AD, including amyloid plaque deposition, synaptic deficits, learning and memory impairments, and other behavioral abnormalities (Games et al., 1995; Hsiao et al., 1996; Hsia et al., 1999; Palop et al., 2003; Götz et al., 2004; Kobayashi and Chen, 2005). Pathogenic Aβ assemblies elicit aberrant excitatory activity in cortical-hippocampal networks and compensatory responses that are particularly evident in the DG (Palop et al., 2003; Palop et al., 2005; Palop et al., 2007).

It is unclear which brain regions or cell types are first affected by APP/Aβ to ultimately elicit this network dysfunction. AD has been proposed to "spread" through anatomically and functionally connected brain regions (Braak and Braak, 1991; Buckner et al., 2005; Braak et al., 2006), perhaps by a prion-like mechanism (Eisele et al., 2009; Frost and Diamond, 2010). In human patients, the EC is an early target and could be the region from where AD invades other brain regions. Neuronal alterations starting in the EC could propagate throughout EC-hippocampal-cortical networks. It has been hypothesized that AD originates in the EC because APP expression was found to be higher in layer II neurons of the EC than in other cortical areas in cognitively intact people (Roberts et al., 1993). Levels further increased in early-stage AD but declined in late stages (Roberts et al., 1993). However, more recent studies have not found higher APP levels in EC neurons of cognitively intact individuals, and found no difference in expression in patients with mid- to late-stage AD (Liang et al., 2007; Liang et al., 2008).

Given its various effects on synaptic function (Palop and Mucke, 2010), Aβ could be the key mediator of the proposed transsynaptic (i.e., across a synapse) progression of AD. To assess whether production of human Aβ by EC neurons can elicit AD-like behavioral deficits and cortical-hippocampal network dysfunction, we analyzed mice in which transgene-derived APP expression was limited primarily to neurons of the superficial layers of the EC and the pre-/para-subiculum. Predominant expression of APP/Aβ in layer II/III neurons of the EC caused behavioral deficits such as disinhibition and hyperactivity, and age-related cognitive deficits in spatial learning and memory tasks. Similar behavioral phenotypes have been described in transgenic mice with widespread neuronal expression of APP/Aβ (Palop et al., 2003; Götz et al., 2004; Chin et al., 2005; Kobayashi and Chen, 2005; Cheng et al., 2007). Soluble Aβ levels were high in the DG of young mice with APP/Aβ expression in EC neurons, suggesting presynaptic synthesis and/or release of Aβ. In addition, deposits of Aβ in the hippocampus of older mice were mostly seen in perforant pathway terminal fields. Finally, selective overexpression of APP/Aβ in EC neurons also increased cortical network excitability, synaptic loss in the outer molecular layer of the DG, and alterations in synaptic-activity related molecules within granule cells of the DG that typically reflect such aberrant network activity.

RESULTS

Expression of APP in the EC of Neuropsin-tTA/tet-APP Doubly Transgenic (EC-APP) Mice

We produced mice with regionally selective overexpression of APP carrying familial AD mutations by breeding neuropsin-tTA transgenic mice (Yasuda and Mayford, 2006) with tet-APP transgenic mice (Jankowsky et al., 2005) (Figure 1A). The tet-APP transgene encodes a chimeric mouse APP with a humanized Aβ domain (Jankowsky et al., 2005). None of the mice were treated with doxycycline, allowing for the transactivation of tet-APP expression by tTA. Offspring carrying both transgenes (EC-APP mice) expressed mutant APP primarily in the parahippocampal cortex, including the medial EC and pre/para-subiculum (Figure 1B–D). This pattern is in stark contrast to the spatially generalized expression pattern of APP in previously established APP transgenic lines, such as the human APP (hAPP) transgenic line J20 (Figure S1A,B). The expression pattern of mutant APP in EC-APP mice was consistent with that of other tet-regulatable transgenes after crosses with the neuropsin-tTA line (Yasuda and Mayford, 2006). However, we observed some additional transgene expression in the lateral EC, as well as scattered cells with faint expression in superficial layers of other cortical regions and in area CA of the hippocampus (Figure 1B–D and Figure S2). No mutant APP was detected in NTG or singly tTA transgenic mice, and only very low levels of mutant APP in the CA region of tet-APP singly transgenic mice, suggesting minimal “leakiness” of transgene expression in the absence of tTA (Figure S3A,B). Cells expressing mutant APP in the EC were mostly layer II or III neurons (Figure 1D, middle). No mutant APP was detected in granule cells of the DG, although some scattered APP-positive cells were seen in the hilus (Figure 1D, right).

Measurement of mutant APP levels in microdissected brain regions by western blotting confirmed the immunohistochemical analyses. The EC had the highest level of full-length mutant APP, with lower levels seen in the DG (13%) and CA (25%) regions (Figure 1E,F). These levels were not significantly different from the “leaky” expression detected in tet-APP singly transgenic mice (Figure S3). The retrosplenial/posterior cingulate cortex (RC), which also showed some immunostaining for mutant APP (Figure 1B), had ~36% of the expression levels in the EC (Figure 1F).

To ensure that the immunohistochemical staining accurately identified cells in which transgene-derived APP mRNA was synthesized, we performed *in situ* hybridization with an oligonucleotide probe that specifically recognizes APP mRNA encoding the human Aβ domain. The pattern of transgene-derived APP mRNA expression matched the immunostaining pattern obtained with the anti-human Aβ antibody 6E10 (Figure S4). Transgene expression in the EC was higher in EC-APP mice than in hAPP-J20 mice, whose transgene expression levels were highest in the DG (Figures S1C,D and S4C).

Expression of Mutant APP Predominantly in the EC Impairs Spatial Learning and Memory

Spatial learning and memory was examined in the Morris water maze (MWM). At different ages, mice were trained over 5 consecutive days to navigate to a hidden platform using spatial cues outside the maze. At 4 months, EC-APP (tTA/tet) mice and control groups (NTG, tTA and tet-APP) did not differ in their ability to learn this task, as reflected in the total distance covered (Figure 2A) to reach the target platform. EC-APP mice displayed a trend toward delayed acquisition in the first 2 days of training at 4 months. By 9 months of age, the same EC-APP mice were significantly impaired relative to all control groups in acquiring this task (Figure 2B). Mice were trained in the water maze once more at 13 months of age using a protocol shortened to 3 days. EC-APP mice continued to have spatial learning deficits at this age (Figure 2C). Latency to reach the target platform revealed similar differences among groups (data not shown). Swim speeds during hidden platform

training were not different among the groups of mice, and all groups performed equally well in the cued version of the task (data not shown).

The target platform was removed 24 h after the last day of hidden training to assess memory retention at each age. At 4 months, all groups of mice spent more time searching in the target quadrant (where the platform had been located) than in the other quadrants, indicating good memory retention (Figure 2D). At 9 months, all control groups, but not EC-APP mice, showed a significant preference for the target quadrant (Figure 2E). By 13 months, the control groups still favored the target quadrant, whereas EC-APP mice showed no preference for the target quadrant, indicating very poor spatial memory (Figure 2F).

Next, we analyzed spatial reversal learning in 13-month-old mice. For this test, the target platform was moved to a new location 24 h after the probe trial that followed the initial hidden platform training. Mice were trained to find this new location for 3 consecutive days. Over time, all control groups, but not EC-APP mice, showed significant improvements during reversal training (Figure 2G). EC-APP mice were the only group that did not swim shorter distances in the last session than in the first (Figure 2H). The learning and retention deficits shown in the initial component of the water maze testing (Figure 2C,F) complicate the interpretation of this reversal-learning deficit. However, the downward slope of their first learning curves suggests that EC-APP mice learned this task initially, albeit less well than the control groups (Figure 2C, $p=0.06$, ANOVA effect of time), but had no ability to learn in the reversal paradigm.

Expression of Mutant APP Predominantly in the EC Causes Additional Behavioral Abnormalities

Decreased time spent in the open arms of an elevated plus maze is a measure of increased anxiety (Belzung and Griebel, 2001). Several lines of hAPP transgenic mice spend more time in the open arms than NTG controls, suggesting lower levels of anxiety or disinhibition (Chin et al., 2005; Ognibene et al., 2005; Cheng et al., 2007; Roberson et al., 2007; Meilandt et al., 2009). Like transgenic mice with widespread expression of hAPP, EC-APP mice spent significantly more time in the open arms than the control groups at all ages (Figure 3A–C). All groups of mice showed some habituation to the elevated plus maze with repeated testing (Figure 3D).

Different lines of hAPP transgenic mice also show hyperactivity in several arenas, including the open field and Y-maze (Chin et al., 2005; Kobayashi and Chen, 2005; Cheng et al., 2007; Roberson et al., 2007; Meilandt et al., 2009). At 9 months, EC-APP mice showed a trend toward increased total activity in the Y-maze (Figure 3E). By 13 months, EC-APP mice were clearly hyperactive compared with control groups (Figure 3F). There was no habituation of total activity levels to repeated Y-maze testing in any group (3G). EC-APP mice were not impaired in the working memory component of the Y-maze (data not shown). Unlike transgenic lines with widespread hAPP expression, EC-APP mice showed no alterations in locomotor activity in the open field at any age (Figure S5).

Expression of Mutant APP Predominantly in the EC Elicits Alterations in Calcium- And Synaptic Activity–Related Proteins in the DG

Our previous studies in hAPP-J20 mice identified strong correlations between learning and memory deficits and depletions of calbindin-D_{28K} and Fos in granule cells of the DG (Palop et al., 2003; Chin et al., 2005; Cheng et al., 2007; Roberson et al., 2007; Meilandt et al., 2008). In addition, DG granule cells of hAPP-J20 mice ectopically express neuropeptide Y (NPY) in the mossy fiber pathway to CA3 (Palop et al., 2007). NPY levels are also increased in the DG molecular layer of hAPP-J20 mice, likely a result of enhanced

expression by interneurons (Palop et al., 2007). Most of these DG-specific molecular alterations are probably compensatory responses to Aβ-induced aberrant network activity (Palop et al., 2007).

To determine whether alterations in these proteins are caused by APP/Aβ expression in the EC, we measured their levels in the DG of two groups of EC-APP mice (Figure 4): 6-month-old naive mice that had never been tested behaviorally and mice that were tested at 4, 9, and 13 months. Although EC-APP mice had no transgene-derived APP in DG granule cells (Figure 1), they had lower calbindin levels in the molecular layer at 6 and 13 months than age-matched controls (Figure 4A,B). The number of granule cells expressing Fos was also reduced at both ages (Figure 4C,D), and there was a subtle, but significant, increase in NPY expression in the mossy fibers (Figure 4E,F). NPY expression in the molecular layer of the DG was unchanged (data not shown), suggesting that expression of APP/Aβ in the EC and perforant pathway selectively affects granule cells but not interneurons in the DG.

Expression of Mutant APP Predominantly in the EC Induces Abnormal Network Excitability

EEG recordings in other lines of APP transgenic mice revealed cortical and hippocampal epileptic activity (Palop et al., 2007; Minkeviciene et al., 2009). Since EC-APP mice displayed several molecular changes in the DG that indicate such network alterations (Figure 4; (Palop et al., 2003; Palop et al., 2007), we hypothesized that these mice would also have periods of aberrant excitatory neuronal activity. To test this hypothesis, we used video and EEG recordings to monitor EC-APP and control groups of mice at 4–5 months of age over 24 h. Bilateral recording electrodes over the parietal cortex (PC) revealed very few or no sharp wave discharges (SWDs) in control mice (Figure 5A–C, F) and an average of 30 SWDs per hour in EC-APP mice (Figure 5D–F). No seizures occurred. Thus, EC-APP mice have widespread cortical network alterations, even though mutant APP expression is restricted primarily to the EC. After the recordings, we confirmed that the mice had no Aβ deposition in the PC (data not shown).

Synaptic Deficits in EC-APP Mice

Loss of synaptophysin-immunoreactive presynaptic terminals in specific brain regions is a characteristic feature of AD pathology that correlates well with the degree of cognitive impairments (Terry et al., 1991; Sze et al., 1997). Several hAPP transgenic lines, including line J20, show similar synaptic alterations (Hsia et al., 1999; Mucke et al., 2000; Chin et al., 2004; Galvan et al., 2006; Tomiyama et al., 2010). In 6- and 13-month-old EC-APP mice, significant synaptophysin loss was observed in the outer molecular layer of the DG, a terminal field of the perforant path (Figure 6A,B). Compared with NTG mice, EC-APP mice also showed a loss of synaptophysin in the stratum radiatum of CA1, where the Schaffer collaterals terminate, but it was more subtle and detectable only at 13 months (Figure 6C,D). Thus, at older ages some synaptic loss may occur downstream of the initial impairment of the perforant path to granule cell synapse.

To determine whether expression of mutant APP in the EC also impairs synaptic functions in the hippocampus, we measured long-term potentiation (LTP) and baseline synaptic transmission at perforant path to granule cell synapses and at the Schaffer collateral synapses in CA1. hAPP-J20 mice show distinct electrophysiological abnormalities at different synapses (Palop et al., 2007; Sun et al., 2008; Harris et al., 2010). Specifically, the perforant path to granule cell synapses show impairments in LTP, but not baseline synaptic transmission. In contrast, the Schaffer collateral synapses onto CA1 pyramidal cells have baseline synaptic transmission deficits, but normal LTP. Recording of extracellular field excitatory post-synaptic potential (fEPSP) revealed no abnormalities in these measures at either synapse in 6-month-old EC-APP mice (data not shown). Therefore, we measured LTP

and baseline synaptic transmission in mice with well-developed cognitive deficits. We first tested a new cohort of NTG and EC-APP mice at 13–14 months of age in the MWM, and replicated the learning and memory deficits described in Figure 2 (data not shown). In EC-APP mice with verified spatial learning deficits, baseline synaptic transmission strength was reduced at Schaffer collateral to CA1 synapses, but not perforant path to granule cell synapses (Figure 6E,F). As in hAPP-J20 mice, LTP was depressed at perforant path to granule cell synapses in EC-APP mice relative to NTG controls, but no LTP deficits were identified in CA1 (Figure 6G,H).

Aβ Deposition in EC-APP Mice

Molecular alterations in DG granule cells of EC-APP mice could result from direct actions of presynaptically released Aβ on postsynaptic membranes or from functional changes in afferent input from perforant path axons caused by Aβ in EC neurons. To address these nonexclusive possibilities, we determined whether Aβ was present not only in the EC, but also in terminal projection zones of EC layer II/III neurons, which overexpress APP/Aβ in EC-APP mice. Soluble Aβ was measured by ELISA in microdissected brain regions of young EC-APP mice before plaque deposition and compared to hAPP-J20 mice. EC-APP mice had high levels of Aβ1-x and Aβ1–42 in the EC (Figure 7A) and relatively high levels of Aβ1-x in the DG (Figure 7B), comparable to those of hAPP-J20 mice, which have much higher APP levels in the DG (Figure S1C,D). In contrast, levels of Aβ1–42 in the DG (Figure 7B) and of Aβ1-x and Aβ1–42 in the CA1 region (Figure 7C) were lower in EC-APP mice than in hAPP-J20 mice. EC-APP mice had higher levels of soluble Aβ in EC and DG, but not CA regions (Figure S3C–E), than singly transgenic tet-APP mice. Therefore, the low levels of Aβ in the CA of young EC-APP mice were likely caused by leakiness of the tet promoter.

At 6 months of age, EC-APP mice had Aβ-immunoreactive deposits in the EC and the RC, but not in other cortical areas or in the DG (Figure 7D). By 13 months, Aβ deposition had increased markedly in the EC and RC and in the DG and CA regions of the hippocampus. Aβ deposition also increased in the PC, which is near the RC (Figure 7E,F). The extent of Aβ deposition in the EC and RC was comparable and significantly higher than in the other regions analyzed. Aβ deposits were found in all layers in the EC (Figure 7F, left) and primarily in the perforant pathway terminal fields in the hippocampus: the stratum lacunosum moleculare (Figure 7F, middle) and the molecular layer of the DG (Figure 7F, right). Aβ deposits were minimal or absent in the hilus and mossy fiber pathway. In contrast, hAPP-J20 mice had particularly prominent deposits in the inner molecular layer of the DG and mossy fiber pathway in CA3 (Figure S6). This pattern of deposition in EC-APP mice strongly suggests presynaptic release of Aβ, as opposed to simple diffusion from the EC.

Finally, we measured the levels of smaller, potentially more toxic, oligomeric Aβ assemblies in the EC, DG, and CA1 of 13-month-old EC-APP mice by immunoprecipitation and western blotting. The intensity of bands corresponding to Aβ dimers was most intense in EC, intermediate in DG, and lowest in CA1 (Figure 7G,H). Aβ dimer levels in DG were comparable in EC-APP and hAPP-J20 mice (Figure 7G), but Aβ monomer levels in DG and CA1 were lower in EC-APP mice.

Reducing Aβ Production by γ-Secretase Inhibition Reverses an Abnormal Behavior in EC-APP Mice

Much evidence suggests that Aβ is the primary mediator of AD-related molecular and behavioral abnormalities in APP transgenic mice and human patients (Palop et al., 2003; Walsh and Selkoe, 2004; Tanzi, 2005; Palop et al., 2007; Sun et al., 2008; Harris et al., 2010). However, other APP metabolites or the holoprotein itself could also have a role.

Therefore, we analyzed the behavioral effects of LY-411575, a γ-secretase inhibitor (GSI) that rapidly reduces tissue and interstitial fluid levels of Aβ in APP transgenic mice (Cirrito et al., 2003; Lanz et al., 2004; Abramowski et al., 2008). Four-month-old EC-APP and NTG mice were treated once daily for 2 days and tested in the elevated plus maze because it is a quick and sensitive test of dysfunction in this line (Figure 3 and 8A), and chronic treatment with this GSI causes mice to become too ill for long-term behavioral experiments such as the MWM (unpublished observations). LY-411575-treated EC-APP mice spent significantly less time in the open arms of the maze than vehicle-treated EC-APP mice, normalizing their behavior in this test as compared with vehicle-treated NTG controls (Figure 8A). There was a trend toward increased open arm time in NTG mice treated with LY-411575 compared to vehicle-treated NTG controls, but this difference was not statistically significant.

We verified that LY-411575 was active by measuring C-terminal fragments (CTFs) in the EC, which increase when γ-secretase is inhibited (Cirrito et al., 2003; Abramowski et al., 2008). Ten hours after the second injection of LY-411575, CTF levels were significantly increased (Figure 8B). This result makes it very unlikely that β-secretase-cleaved CTFs, such as C99, underlie this behavioral abnormality in APP transgenic mice. Measurements of Aβ levels were not used as a reporter for LY-411575 activity because mice at this age already have Aβ deposition in the EC, and existing plaques are not reduced by LY-411575 (Garcia-Alloza et al., 2009).

DISCUSSION

It is not known how dysfunction specifically of the EC contributes to overall cognitive decline in AD or whether early vulnerability of the EC initiates the spread of dysfunction through interconnected neural networks. To address these questions, we studied a transgenic mouse model with spatially restricted overexpression of mutant APP primarily within the superficial layer neurons of the EC. Our results show that overexpression of mutant APP within the EC causes age-dependent deficits in learning and memory, other behavioral alterations, and aberrant synchronization in distant cortical networks. We also demonstrate that Aβ-induced molecular and functional impairments can cross synapses, progressing with time/aging initially from EC neurons to granule cells in the DG and then to pyramidal neurons in CA1. Our data directly support the hypothesis that AD-related neuronal dysfunction is propagated through synaptically connected neural networks, with the EC as an important hub region of early vulnerability.

Potential Involvement of the Retrosplenial Cortex

In AD, PiB-PET and fMRI studies demonstrated extensive Aβ deposition in the “default mode network” (DMN), a group of brain regions with correlative activity that deactivate during cognitive tasks (Buckner et al., 2005; Sperling et al., 2009). One major hub of the DMN is the posterior cingulate cortex (Buckner et al., 2005), which includes the RC in humans and nonhuman primates (Vann et al., 2009). Reminiscent of the human imaging studies, we found extensive Aβ deposition in the RC of EC-APP mice, which was not different from that in the EC, even though APP overexpression was much lower in the RC than the EC (Figure 1). hAPP-J20 mice also had substantial Aβ deposition in the RC (Supplemental Figure 6).

The RC has reciprocal connections to the medial EC (Wyss and Van Groen, 1992; Van Groen and Wyss, 2003; Jones and Witter, 2007), but inputs from the medial EC originate in neurons of deeper layers (Insausti et al., 1997), not in neurons of superficial layers, which express mutant APP in the EC-APP mouse model. Thus, the EC is an unlikely source of Aβ deposition in the RC of these mice. EC-APP mice also express mutant APP in the parahippocampal pre- and para-subiculum, which have reciprocal connections to the RC

(Wyss and Van Groen, 1992; Van Groen and Wyss, 2003; Jones and Witter, 2007). Therefore, presynaptic terminals from these regions may release Aβ into the RC. The RC also receives hippocampal input directly from the subiculum, but does not share direct projections with the DG, CA1, or CA3, at least in rats (van Groen and Wyss, 1990, 1992; Wyss and Van Groen, 1992; Van Groen and Wyss, 2003; Jones and Witter, 2007). In light of these anatomical connections, neurons of the RC could also be affected indirectly by Aβ-induced alterations in the activity of the EC-hippocampal network. Indeed, lesions of the hippocampus reduce immediate-early gene expression in the RC (Albasser et al., 2007).

In conjunction with the hippocampus, the RC plays an important role in spatial navigation, learning, and memory in rodents and humans (Vann et al., 2009). Therefore, accumulation of pathogenic Aβ assemblies in the RC could contribute directly to deficits in these functions. Importantly, the EC, RC, and hippocampus are part of a broader network regulating spatial learning and memory, and dysfunction in one region is not necessarily independent of dysfunction in the others.

Transsynaptic Effects of Aβ

Lesions of the EC or transecting the perforant pathway reduces Aβ deposition in the DG of transgenic APP/PS1 mice (Lazarov et al., 2002; Sheng et al., 2002). These studies support the hypothesis that the EC is a primary source of Aβ in the hippocampus. However, because neuronal activity increases Aβ production (Kamenetz et al., 2003; Cirrito et al., 2005; Cirrito et al., 2008), reduced Aβ deposition in the DG after perforant pathway lesions might also result from decreased stimulation of granule cells in the DG and commensurate decreases in their activity and Aβ production. Our data directly demonstrate that perforant pathway axons are an important source of Aβ in the DG, since APP expression in EC-APP mice was seen in the EC and perforant path but not in DG granule cells. These findings are consistent with other data suggesting that presynaptic terminals are a key site for the production and release of Aβ (Buxbaum et al., 1998; Wei et al., 2010).

Aβ released from perforant pathway terminals may act directly on postsynaptic cells and alter their functions, particularly when aggregated in oligomeric assemblies. Alternatively, Aβ may affect the presynaptic terminals themselves, for instance, by altering the release probability of synaptic vesicles (Abramov et al., 2009) and, thus, changing downstream signaling pathways in the postsynaptic granule cells. In addition, Aβ synthesized and released from cell bodies or dendrites of EC neurons may act on these very cells, causing alterations in afferent input to the DG. These possibilities are not mutually exclusive and deserve to be explored in future studies. The reduction in synaptic activity-related proteins in DG granule cells probably reflects altered network properties and could have detrimental effects on hippocampal function. For example, reducing calbindin or Fos levels in normal rats or mice causes deficits in spatial learning tasks (Molinari et al., 1996; He et al., 2002); decreased levels of synaptophysin suggest loss or impairment of presynaptic terminals that could disrupt communication between the EC and DG (Terry et al., 1991; Hsia et al., 1999; Scheff and Price, 2003).

Independent of whether Aβ exerts its main effects in the EC, DG, or both, the progression of molecular and functional synaptic alterations from EC neurons to DG neurons and CA1 neurons strongly support the hypothesis that AD progresses through synaptically connected neural networks and that this process is triggered in good part by Aβ (Braak and Braak, 1991; Buckner et al., 2005; Braak et al., 2006; Palop et al., 2006; Palop and Mucke, 2009; Seeley et al., 2009; Sperling et al., 2009). The propagation of functional alterations into the DG and CA1 are likely to be very rapid, whereas molecular and structural changes may require more time to develop as suggested by the delayed decrease in synaptophysin levels

in CA1. Whether APP/Aβ expression in the EC exerts indirect effects on DG target cells in the hilus or CA3 region remains to be determined.

Similarities between hippocampal synaptic deficits in hAPP-J20 mice with high levels of Aβ in DG and CA1, and in EC-APP mice with lower levels of Aβ in these regions suggest two possibilities. First, the deficits may emerge whenever Aβ levels exceed a certain threshold. In support of this possibility, synaptic transmission deficits in CA1 are also present in hAPP-J9 mice, whose hippocampal hAPP/Aβ levels are half those in hAPP-J20 mice (Hsia et al., 1999; Mucke et al., 2000). Aβ levels in the DG of EC-APP mice (representing Aβ released from EC-derived terminals) are ~70% of those in hAPP-J20 mice (Figure 7B). Second, synaptic deficits in the hippocampus of both lines may be caused indirectly by Aβ-induced abnormalities in the activity of EC neurons. These possibilities are not mutually exclusive. The detection of epileptiform activity in the parietal cortex of EC-APP mice suggests that APP/Aβ in one area may impact other brain regions by causing aberrant activity patterns that rapidly spread through interconnected neural networks.

Aβ is released from presynaptic terminals (Wei et al., 2010) and, in our opinion, is the likeliest APP metabolite to mediate transsynaptic spread of AD. The caspase-generated APP-C31 fragment (Gervais et al., 1999; Weidemann et al., 1999) does not play a major role in the development of AD-related abnormalities in APP transgenic mice (Harris et al., 2010). Treatment with the γ-secretase inhibitor LY-411575, which decreases soluble Aβ levels (Cirrito et al., 2003; Lanz et al., 2004; Abramowski et al., 2008) and increases CTF levels (Figure 8B) (Cirrito et al., 2003; Abramowski et al., 2008), reversed behavioral abnormalities in EC-APP mice. This finding supports a critical role of Aβ and makes it very unlikely that the abnormal behavior of EC-APP mice was caused by β-secretase-cleaved CTFs such as C99. However, it does not exclude potential contributions from all other APP metabolites that might have co-pathogenic effects, including N-APP (Nikolaev et al., 2009) and AICD (Ghosal et al., 2009).

Role of the EC in Cognitive and Noncognitive Behaviors

Although the relationship between cognitive and behavioral abnormalities in APP transgenic mice and humans with AD is a matter of debate, we previously identified prominent navigational and hippocampal deficits in both the models and in AD patients (deIpolyi et al., 2007; deIpolyi et al., 2008). In the current study, increasing Aβ production by EC neurons, and perhaps also by RC neurons, caused age-dependent deficits in spatial learning and memory, suggesting that impairments of those neurons or their target regions are critical for the functional deficits. Indeed, the EC and its intact perforant path connections to the hippocampus are critical for learning, retrieval, and/or consolidation of spatial memory (Kirkby and Higgins, 1998; Remondes and Schuman, 2004; Steffenach et al., 2005; Ramirez et al., 2007), and working memory (Kirkby and Higgins, 1998). Aβ-induced dysfunction of the RC could also contribute to these behavioral deficits (Vann et al., 2009).

The reversal-learning paradigm (Figure 2G,H) provides new evidence for a specific role of the EC and its connections in flexible learning of a new spatial task. This task requires mice to discard a previously learned target location and to acquire a new one. EC-APP mice had difficulties learning the new platform location. The learning deficits in the initial component of the water maze complicate the interpretation of this phenotype as solely a reversal-learning deficit. However, while EC-APP mice did not show significant memory retention in the first task, they did show some evidence of learning to navigate to the hidden platform initially (Figure 2C, $p=0.06$, one-way ANOVA effect of time). The lack of any improvement in the reversal-learning task suggests an additional impairment in flexibility or reflects other behavioral disturbances. The EC-APP model could help elucidate the roles of the EC and perforant pathway projections in this process.

Mice of the APP transgenic line PDAPP 109 were also impaired in a related behavioral task (Chen et al., 2000). Neither the anatomical regions nor the molecular mechanisms underlying the required flexibility have been elucidated, although a recent study found adult neurogenesis in the DG to be important for spatial reversal learning (Garthe et al., 2009). Adult neurogenesis in the DG is altered in APP transgenic mice (Haughey et al., 2002; Donovan et al., 2006; Lopez-Toledano and Shelanski, 2007; Verret et al., 2007; Sun et al., 2009), most likely because Aβ causes an imbalance in excitatory and inhibitory inputs to newborn granule cells (Sun et al., 2009).

In addition to deficits in spatial learning and memory, EC-APP mice behaved abnormally in the elevated plus maze and were hyperactive in the Y-maze. Time spent in the open arms of an elevated plus maze is usually considered a measure of anxiety, and, with this interpretation, several lines of hAPP mice appear to be less anxious (Chin et al., 2005; Ognibene et al., 2005; Cheng et al., 2007; Roberson et al., 2007; Meilandt et al., 2009; Harris et al., 2010). Increased time spent in the open arms could also reflect disinhibition in APP transgenic mice (Ognibene et al., 2005; Meilandt et al., 2009; Harris et al., 2010). The amygdala, regarded as the anatomical substrate of fear and anxiety-related behaviors, receives direct input from the EC. However, this input is from neurons in deep cortical layers (McDonald, 1998), which do not overexpress mutant APP in the EC-APP mice. The ventral hippocampus is more specifically associated with performance in the elevated plus maze than the amygdala (Bannerman et al., 2004) and receives direct input from the superficial layer neurons overexpressing mutant APP in EC-APP mice. Similar to what we observed in EC-APP mice, rats with lesions of the ventral hippocampus, or severed perforant pathway projections to the ventral hippocampus, spent more time in the open arms of an elevated plus maze (Kjelstrup et al., 2002; Steffenach et al., 2005). Our data further support a role of the EC and its hippocampal connections in the etiology of this behavioral phenotype, although the amygdala could still be involved in a more indirect fashion.

The hippocampus has also been implicated as one of many brain regions that can regulate locomotor activity (Bast and Feldon, 2003). Unlike APP transgenic mice with widespread transgene expression, which are hyperactive in both the open field and the Y-maze (Chin et al., 2005; Kobayashi and Chen, 2005; Roberson et al., 2007), EC-APP mice were hyperactive only in the Y-maze. Why EC-APP mice performed differently in these tests is unclear, but this dissociation suggests that these tests measure different components of locomotor activity control. In further support of this conclusion, all groups of mice habituated to the open field, but not to the Y-maze. Activity in the open field may be related to hippocampus-dependent information gathering about a novel environment, whereas locomotor activity in the Y-maze may reflect a different process.

Therapeutic Implications

Because effective drug treatments for AD are lacking, interest has been increasing in alternative approaches, such as gene therapy and stem cells (Tuszynski et al., 2005; Spencer et al., 2007). However, the success of these approaches may depend on whether AD affects multiple brain regions in parallel or in sequence. In the latter case, its progression might be stopped by targeting the specific region in which the disease originates, which would be simpler than targeting multiple regions. Thus, if dysfunction in the EC leads to the propagation of AD across synapses throughout a neural network, early interference specifically in the EC might be of therapeutic benefit, perhaps halting disease progression. Indeed, BDNF introduced into the EC was transported into the hippocampus and rescued spatial memory functions in APP transgenic mice (Nagahara et al., 2009). Tau and Aβ may also share features with prions, including the ability to propagate pathological protein aggregation, perhaps through synaptic connections (Meyer-Luehmann et al., 2006; Clavaguera et al., 2009; Eisele et al., 2009; Frost et al., 2009; Frost and Diamond, 2010). It

will be interesting to assess the effects of selective EC expression of tau and other factors on the development and propagation of AD-related pathologies.

EXPERIMENTAL PROCEDURES

Animals

Neuropsin-tTA heterozygous transgenic mice (Yasuda and Mayford, 2006) were crossed with tet-APP heterozygous transgenic mice (Jankowsky et al., 2005) to generate four genotypes: tTA/tet doubly transgenic (EC-APP) mice, tTA or tet singly transgenic mice, and NTG controls. Mice did not receive doxycycline so as to maintain expression of the tet-APP transgene. Neuropsin-tTA mice on the C57BL6 background were kindly provided by Dr. Mark Mayford. Tet-APP mice (Jackson Laboratory) were on a C57BL6/C3H background (stock #006004) or after backcrossing for >10 generations onto a C57BL6 background (stock #007049). Because C57BL6/C3H tet-APP mice were available first, most data were obtained on this background. However, soluble Aβ measurements in 3-month-old mice, detection of oligomers in 13-month-old mice, electrophysiological and EEG recordings were performed on the pure C57BL/6 background. Immunohistochemical and western blot analyses of EC-APP mice on the C57BL/6 or C57BL6/C3H background yielded comparable results (data not shown). All analyses were done in gender-balanced groups. The experimenters were blinded to genotype and treatment for these studies. The Institutional Animal Care and Use Committee of the University of California, San Francisco approved all experiments.

Behavioral Tests

One cohort of mice was evaluated at 4, 9, and 13 months of age in the elevated plus maze and MWM. The same mice were analyzed in the Y-maze at 9 and 13 months.

Elevated Plus Maze

The elevated plus maze consisted of two open (without walls) and two enclosed (with walls) arms elevated 63 cm above the ground (Hamilton-Kinder, Poway, CA). Mice were allowed to habituate in the testing room under dim light for 1 h before testing. During testing, mice were placed at the junction between the open and closed arms of the plus maze and allowed to explore for 5 min. The maze was cleaned with 70% alcohol after testing of each mouse. Total distance traveled and time spent in the open and closed arms were calculated based on infrared photobeam breaks.

Y-Maze

The apparatus consisted of three symmetrical arms in the shape of a Y. Before testing, mice were transferred to the testing room and acclimated for at least 1 h. During testing, each mouse was placed in a starting arm facing the wall and arm entries were recorded for 6 minutes, divided into six 1-min intervals. The maze was cleaned with 70% alcohol between testing of each mouse. Spontaneous alternations and total activity were calculated.

Morris Water Maze

The water maze consisted of a pool (122 cm diameter) filled with water (21±1°C) made opaque with nontoxic white powder. The pool was surrounded by distinct extra-maze (spatial) cues. Before hidden platform training, mice were given four pre-training trials in which they had to swim in a rectangular channel (15 cm × 122 cm) and mount a platform submerged 1.5 cm in the middle of the channel. Mice that did not mount the platform within 90 s were guided to it and allowed to sit on it for 10 s. The day after pre-training, mice were trained in the circular water maze.

For hidden platform training, the platform (14 cm × 14 cm) was submerged 1.5 cm. The platform location remained the same, but the drop location varied semi-randomly between trials. Mice that did not find the platform within 60 s were guided to it and allowed to sit on it for 10 s. At 4 and 9 months of age, mice received two training sessions with 3-h inter-session intervals for five consecutive days. Each session consisted of two trials with 10 min inter-trial intervals. At 13 months, mice were trained for only 3 days followed by reversal training (see below). Spatial probe trials, during which the platform was removed and mice were allowed to swim for 60 s before they were removed, were carried out 24 h after hidden platform training. For these trials, the drop location was 180° from where the platform was placed during hidden platform training.

For reversal training, the target platform was moved to the opposite quadrant 24 h after the probe trial and mice were trained to the new target location as above for three consecutive days. Another probe trial was given 24 h after the last hidden reversal session.

Behavior was recorded with a video tracking system (Noldus). Escape latencies, distance traveled, swim paths, swim speeds, percent time spent in each quadrant, and platform crossings were recorded for subsequent analysis. Thigmotaxis behavior was monitored during the last trial of hidden platform training in both initial acquisition and reversal-learning. No mice exhibited thigmotaxis in these experiments. Floating behavior was also monitored during training. Only one mouse (a singly tTA transgenic at 13 months) exhibited floating and was removed from the analysis.

γ-Secretase Inhibitor Treatment

NTG and EC-APP mice were injected subcutaneously once daily for 2 days with 3 mg/kg LY-411575 (a generous gift of Dr. J. Tung and the Myelin Repair Foundation, Saratoga, CA) or vehicle (corn oil). Six to 8 h after the last injection, mice were tested in the elevated plus maze. All mice were sacrificed directly after the elevated plus maze (approximately 10 h from the second LY-411575 injection), and brains were harvested and frozen for ELISA and Western blot analyses.

Immunohistochemistry

Mice were anesthetized with Avertin (250 mg/kg; 2,2,2-tribromoethanol dissolved in tert-amyl alcohol and PBS) and transcardially perfused with 0.9% saline. One hemibrain was drop-fixed in 4% paraformaldehyde for 48 h and the other hemibrain immediately frozen at −70°C. Coronal sections (30 μm) were prepared with a sliding microtome and collected for immunohistochemistry. Primary antibodies were rabbit anti-calbindin (1:20,000; Swant, Bellinzona, Switzerland), rabbit anti-Fos (1:10,000; Ab-5, Oncogene, San Diego, CA), rabbit anti-NPY (1:8,000; Immunostar, Hudson, WI), mouse biotinylated anti-Aβ (1:400; 3D6, Elan Pharmaceuticals, South San Francisco, CA), mouse anti-APP/Aβ (1:10,000; clone 6E10; Covance, Princeton, NJ) mouse anti-hAPP (1:2000, clone 8E5, Elan Pharmaceuticals), and mouse anti-synaptophysin (1:1000; Boehringer Mannheim, Indianapolis, IN). Sections labeled with anti-synaptophysin were incubated with FITC-conjugated horse anti-mouse IgG secondary antibody (1:75; Vector Laboratories, Burlingame, CA). Binding of other primary antibodies was detected with biotinylated donkey anti-rabbit or anti-mouse (1:1000; Jackson Immunoresearch Laboratories, West Grove, PA), followed by incubation with avidin-biotin complex (Vector Laboratories). Diaminobenzidine was used as the chromagen. Fos, calbindin, NPY, synaptophysin, and Aβ immunoreactivities were quantified in a behaviorally naive cohort of mice at 6 months and in mice that underwent behavioral testing at 13 months of age. Quantifications were performed as described (Mucke et al., 1995; Palop et al., 2003; Chin et al., 2004; Chin et al., 2005; Palop et al., 2005; Palop et al., 2007; Harris et al., 2010).

Aβ ELISAs and Immunoblotting

For Aβ and APP measurements in specific regions, brain tissues were microdissected into DG, EC, CA, and RC. To obtain DG samples, the granule cell and molecular layers were microdissected away from the hilar region and CA3. For Aβ ELISAs, samples were snap-frozen and homogenized in 5 M guanidine buffer. Aβ1-x (approximates total Aβ) and Aβ1–42 were quantified as described (Johnson-Wood et al., 1997; Mucke et al., 2000). Low-molecular-weight oligomeric Aβ species were detected in microdissected DG, CA1, and EC samples homogenized in buffer containing 0.5 mM EDTA, 1 mM DTT, 0.1 M PMSF, Phosphatase Inhibitor Cocktails I and II (Sigma-Aldrich, St. Louis, MO), and protease inhibitors (Roche, Indianapolis, IN) in PBS. Samples (50 μg) were immunoprecipitated with anti-Aβ1–40 (5C3, 5 μl, Calbiochem, San Diego, CA) and Aβ1–42 (8G7, 5 μl, Calbiochem) antibodies overnight at 4°C. Dimers and trimers of Aβ were then measured by western blotting as described (Chin et al., 2005; Harris et al., 2010) with the additional step of microwaving the nitrocellulose membrane for 2.5 min before blocking in 3% BSA/Tris-buffered saline with 0.5% Tween and incubating with the primary anti-Aβ antibodies. The primary antibody cocktail consisted of 6E10 (1:1000), 4G8 (1:1000, Covance), and 82E1 (1:500, IBL-America, Minneapolis, MN) diluted in 3% BSA/Tris-buffered saline with 0.5% Tween. APP levels were assessed by western blotting in microdissected samples essentially as described (Chin et al., 2005; Harris et al., 2010) with mouse anti-APP/Aβ (1:1000, clone 6E10) and rabbit anti-GAPDH (1:10,000, Sigma-Aldrich) overnight at 4oC. Primary antibodies were detected with HRP-conjugated anti-mouse secondary antibody (1:10,000, Calbiochem) and bands were visualized by ECL. Densitometry measurements of the bands were acquired from scanned images with Quantity One software (Bio-Rad, Hercules, CA).

EEG Recordings

Mice were implanted for video EEG monitoring after anesthesia with intraperitoneal ketamine (75 mg/kg) and medetomidine (1 mg/kg). Teflon-coated silver wire electrodes (0.125-mm diameter) soldered to a multichannel electrical connector were implanted into the subdural space over the left frontal cortex (coordinates relative to bregma were: M/L, ±1, A/P ±1) and the left and right parietal cortex (M/L, ±2, A/P, −2). The left frontal cortex electrode was used as a reference. All EEG recordings were carried out at least 10 days after surgery on freely moving mice in a recording chamber. EEG activity was recorded with the Harmonie software (version 5.0b, Stellate, Canada) for 24 h. The number of sharp-wave discharges was automatically detected by the Gotman spike and seizure detectors (Harmonie, Stellate) and manually verified.

Electrophysiological Recordings in Acute Slices

At 6 and 14 months of age, NTG and EC-APP mice were anesthetized with Avertin or isoflurane and decapitated. The brains were quickly removed and placed in ice-cold solution containing (in mM) 2.5 KCl, 1.25 $NaPO_4$, 10 $MgSO_4$, 0.5 $CaCl_2$, 26 $NaHCO_3$, 11glucose, and 234 sucrose (pH ~7.4; 305 mOsmol). Coronal slices (400 μm) were cut on a Vibratome, collected in the above solution, and incubated for 30 min in standard artificial cerebrospinal fluid (ACSF; 30°C) containing (in mM): 2.5 KCl, 126 NaCl, 10 glucose, 1.25 NaH_2PO_4, 1 $MgSO_4$, 2 $CaCl_2$, and 26 $NaHCO_3$ (290 mOsmol; when gassed with a mixture of 95% O_2–5% CO_2, the pH ~7.4). The slices were maintainedat room temperature for at least 30 min before recording. No recordings were made from slices more than 5 h after dissection. Individual slices were transferred to a submergedrecording chamber, where they were perfused with ACSF at a rate of 2 ml/min.

fEPSPs were recorded with glass electrodes (~3 MΩ tip resistance) filled with 1 M NaCl and 25 mM HEPES (pH, 7.3) and evoked every 20 s with a bipolar tungsten electrode (FHC, Bowdoin, ME). Recordings were filtered at 2 kHz (−3 dB, eight-pole Bessel), digitally

sampled at 20 kHz with a Multiclamp 700A amplifier (Molecular Devices, Foster City, CA), and acquired with a Digidata-1322A digitizer and pClamp 9.2 software. In CA1, the stimulating electrode was placed in the stratum radiatum at the border of CA3 and CA1, and the recording electrode was placed ~150 μm away in CA1 stratum radiatum. In the DG, the stimulating electrode was placed in the medial perforant path (MPP) in the dorsal blade of the DG, and the recording electrode was also placed in the MPP ~150 μm closer to CA3 than the recording electrode. fEPSPs were recorded in the presence of 50 μM picrotoxin (Tocris). Synaptic transmission strength in the DG and CA1 were assessed by generating input-output (I-O) curves for fEPSPs. For each slice, we measured the fiber volley amplitude and initial slope of the fEPSP responses to a range of stimulation from 25 to 800 μA, and a response curve was generated for both values. Stimulus strength was then adjusted to be ~30% of the maximal fEPSP response for recordings that followed. After a 10 min stable baseline was established, LTP was induced in CA1 by high frequency stimulation (four 100-Hz trains of 100 stimuli every 20 s) and in the DG by theta burst stimulation (a set of 10 bursts repeated 10 times every 15 s; each burst, consisting of four pulses at 100 Hz, was repeated at 5 Hz).

Statistical Analyses

For all data acquisition, experimenters were blinded with respect to the genotype and treatment of mice. Statistical analyses were conducted with GraphPad Prism version 4.0 or 5.0 (La Jolla, CA). Differences between means were analyzed by two-tailed Student's t-test, one-way or two-way ANOVA with post-hoc tests as appropriate. Data were considered significant when $p < 0.05$.

Supplementary Material

Refer to Web version on PubMed Central for supplementary material.

Acknowledgments

This work was supported in part by National Institute of Health grants AG011385 and AG022074 to L.M. and a fellowship from the McBean Foundation to J.H. We thank Dr. Mark Mayford for kindly providing neuropsin-tTA mice; B. Halabisky and M. Howard for help with electrophysiological recordings, A. Holloway for statistical advice; X. Wang and H. Solanoy for technical support; S. Ordway for editorial review; and M. De la Cruz for administrative assistance.

References

Abramov E, Dolev I, Fogel H, Ciccotosto GD, Ruff E, Slutsky I. Amyloid-beta as a positive endogenous regulator of release probability at hippocampal synapses. Nat Neurosci 2009;12:1567–1576. [PubMed: 19935655]

Abramowski D, Wiederhold KH, Furrer U, Jaton AL, Neuenschwander A, Runser MJ, Danner S, Reichwald J, Ammaturo D, Staab D, Stoeckli M, Rueeger H, Neumann U, Staufenbiel M. Dynamics of Abeta turnover and deposition in different beta-amyloid precursor protein transgenic mouse models following gamma-secretase inhibition. J Pharmacol Exp Ther 2008;327:411–424. [PubMed: 18687920]

Albasser MM, Poirier GL, Warburton EC, Aggleton JP. Hippocampal lesions halve immediate-early gene protein counts in retrosplenial cortex: distal dysfunctions in a spatial memory system. Eur J Neurosci 2007;26:1254–1266. [PubMed: 17767503]

Bannerman DM, Rawlins JN, McHugh SB, Deacon RM, Yee BK, Bast T, Zhang WN, Pothuizen HH, Feldon J. Regional dissociations within the hippocampus--memory and anxiety. Neurosci Biobehav Rev 2004;28:273–283. [PubMed: 15225971]

Bast T, Feldon J. Hippocampal modulation of sensorimotor processes. Prog Neurobiol 2003;70:319–345. [PubMed: 12963091]

Belzung C, Griebel G. Measuring normal and pathological anxiety-like behaviour in mice: A review. Behav Brain Res 2001;125:141–149. [PubMed: 11682105]

Blennow K, de Leon MJ, Zetterberg H. Alzheimer's disease. Lancet 2006;368:387–403. [PubMed: 16876668]

Braak H, Braak E. Neuropathological stageing of Alzheimer-related changes. Acta Neuropathol 1991;82:239–259. [PubMed: 1759558]

Braak H, Rüb U, Schultz C, Del Tredici K. Vulnerability of cortical neurons to Alzheimer's and Parkinson's diseases. J Alzheimers Dis 2006;9:35–44. [PubMed: 16914843]

Buckner RL, Snyder AZ, Shannon BJ, LaRossa G, Sachs R, Fotenos AF, Sheline YI, Klunk WE, Mathis CA, Morris JC, Mintun MA. Molecular, structural, and functional characterization of Alzheimer's disease: Evidence for a relationship between default activity, amyloid, and memory. J Neurosci 2005;25:7709–7717. [PubMed: 16120771]

Buxbaum JD, Thinakaran G, Koliatsos V, O'Callahan J, Slunt HH, Price DL, Sisodia SS. Alzheimer amyloid protein precursor in the rat hippocampus: Transport and processing through the perforant path. J Neurosci 1998;18:9629–9637. [PubMed: 9822724]

Chen G, Chen KS, Knox J, Inglis J, Bernard A, Martin SJ, Justice A, McConlogue L, Games D, Freedman SB, Morris RG. A learning deficit related to age and b-amyloid plaques in a mouse model of Alzheimer's disease. Nature 2000;408:975–979. [PubMed: 11140684]

Cheng I, Scearce-Levie K, Legleiter J, Palop J, Gerstein H, Bien-Ly N, Puoliväli J, Lesné S, Ashe K, Muchowski P, Mucke L. Accelerating amyloid-β fibrillization reduces oligomer levels and functional deficits in Alzheimer disease mouse models. J Biol Chem 2007;282:23818–23828. [PubMed: 17548355]

Chin J, Palop JJ, Yu G-Q, Kojima N, Masliah E, Mucke L. Fyn kinase modulates synaptotoxicity, but not aberrant sprouting, in human amyloid precursor protein transgenic mice. J Neurosci 2004;24:4692–4697. [PubMed: 15140940]

Chin J, Palop JJ, Puoliväli J, Massaro C, Bien-Ly N, Gerstein H, Scearce-Levie K, Masliah E, Mucke L. Fyn kinase induces synaptic and cognitive impairments in a transgenic mouse model of Alzheimer's disease. J Neurosci 2005;25:9694–9703. [PubMed: 16237174]

Cirrito JR, Kang JE, Lee J, Stewart FR, Verges DK, Silverio LM, Bu G, Mennerick S, Holtzman DM. Endocytosis is required for synaptic activity-dependent release of amyloid-beta in vivo. Neuron 2008;58:42–51. [PubMed: 18400162]

Cirrito JR, Yamada KA, Finn MB, Sloviter RS, Bales KR, May PC, Schoepp DD, Paul SM, Mennerick S, Holtzman DM. Synaptic activity regulates interstitial fluid amyloid-b levels in vivo. Neuron 2005;48:913–922. [PubMed: 16364896]

Cirrito JR, May PC, O'Dell MA, Taylor JW, Parsadanian M, Cramer JW, Audia JE, Nissen JS, Bales KR, Paul SM, DeMattos RB, Holtzman DM. In vivo assessment of brain interstitial fluid with microdialysis reveals plaque-associated changes in amyloid-beta metabolism and half-life. J Neurosci 2003;23:8844–8853. [PubMed: 14523085]

Clavaguera F, Bolmont T, Crowther RA, Abramowski D, Frank S, Probst A, Fraser G, Stalder AK, Beibel M, Staufenbiel M, Jucker M, Goedert M, Tolnay M. Transmission and spreading of tauopathy in transgenic mouse brain. Nat Cell Biol 2009;11:909–913. [PubMed: 19503072]

deIpolyi AR, Rankin KP, Mucke L, Miller BL, Gorno-Tempini ML. Spatial cognition and the human navigation network in AD and MCI. Neurology 2007;69:986–997. [PubMed: 17785667]

deIpolyi AR, Fang S, Palop JJ, Yu G-Q, Wang X, Mucke L. Altered navigational strategy use and visuospatial deficits in hAPP transgenic mice. Neurobiol Aging 2008;29:253–266. [PubMed: 17126954]

Donovan MH, Yazdani U, Norris RD, Games D, German DC, Eisch AJ. Decreased adult hippocampal neurogenesis in the PDAPP mouse model of Alzheimer's disease. J Comp Neurol 2006;495:70–83. [PubMed: 16432899]

Eichenbaum H, Lipton PA. Towards a functional organization of the medial temporal lobe memory system: role of the parahippocampal and medial entorhinal cortical areas. Hippocampus 2008;18:1314–1324. [PubMed: 19021265]

Eisele YS, Bolmont T, Heikenwalder M, Langer F, Jacobson LH, Yan ZX, Roth K, Aguzzi A, Staufenbiel M, Walker LC, Jucker M. Induction of cerebral beta-amyloidosis: intracerebral versus

systemic Abeta inoculation. Proc Natl Acad Sci USA 2009;106:12926–12931. [PubMed: 19622727]

Frost B, Diamond MI. Prion-like mechanisms in neurodegenerative diseases. Nat Rev Neurosci 2010;11:155–159. [PubMed: 20029438]

Frost B, Jacks RL, Diamond MI. Propagation of tau misfolding from the outside to the inside of a cell. J Biol Chem 2009;284:12845–12852. [PubMed: 19282288]

Galvan V, Gorostiza OF, Banwait S, Ataie M, Logvinova AV, Sitaraman S, Carlson E, Sagi SA, Chevallier N, Jin K, Greenberg DA, Bredesen DE. Reversal of Alzheimer's-like pathology and behavior in human APP transgenic mice by mutation of Asp664. Proc Natl Acad Sci USA 2006;103:7130–7135. [PubMed: 16641106]

Games D, Adams D, Alessandrini R, Barbour R, Berthelette P, Blackwell C, Carr T, Clemens J, Donaldson T, Gillespie F, Guido T, Hagopian S, Johnson-Wood K, Khan K, Lee M, Leibowitz P, Lieberburg I, Little S, Masliah E, McConlogue L, Montoya-Zavala M, Mucke L, Paganini L, Penniman E, Power M, Schenk D, Seubert P, Snyder B, Soriano F, Tan H, Vitale J, Wadsworth S, Wolozin B, Zhao J. Alzheimer-type neuropathology in transgenic mice overexpressing V717F β-amyloid precursor protein. Nature 1995;373:523–527. [PubMed: 7845465]

Garcia-Alloza M, Subramanian M, Thyssen D, Borrelli LA, Fauq A, Das P, Golde TE, Hyman BT, Bacskai BJ. Existing plaques and neuritic abnormalities in APP:PS1 mice are not affected by administration of the gamma-secretase inhibitor LY-411575. Mol Neurodegener 2009;4:19. [PubMed: 19419556]

Garthe A, Behr J, Kempermann G. Adult-generated hippocampal neurons allow the flexible use of spatially precise learning strategies. PLoS One 2009;4:e5464. [PubMed: 19421325]

Gervais FG, Xu D, Robertson GS, Vaillancourt JP, Zhu Y, Huang J, Leblanc A, Smith D, Rigby M, Shearman MS, Clarke EE, Zheng H, Ploeg LHTVD, Ruffolo SC, Thornberry NA, Xanthoudakis S, Zamboni RJ, Roy S, Nicholson DW. Involvement of caspases in proteolytic cleavage of Alzheimer's amyloid-b precursor protein and amyloidogenic Ab peptide formation. Cell 1999;97:395–406. [PubMed: 10319819]

Ghosal K, Vogt DL, Liang M, Shen Y, Lamb BT, Pimplikar SW. Alzheimer's disease-like pathological features in transgenic mice expressing the APP intracellular domain. Proc Natl Acad Sci USA 2009;106:18367–18372. [PubMed: 19837693]

Gomez-Isla T, Price JL, McKeel DW Jr, Morris JC, Growdon JH, Hyman BT. Profound loss of layer II entorhinal cortex neurons occurs in very mild Alzheimer's disease. J Neurosci 1996;16:4491–4500. [PubMed: 8699259]

Götz J, Streffer JR, David D, Schild A, Hoerndli F, Pennanen L, Kurosinski P, Chen F. Transgenic animal models of Alzheimer's disease and related disorders: Histopathology, behavior and therapy. Mol Psychiatry 2004;9:664–683. [PubMed: 15052274]

Harris JA, Devidze N, Halabisky B, Lo I, Thwin MT, Yu GQ, Bredesen DE, Masliah E, Mucke L. Many neuronal and behavioral impairments in transgenic mouse models of Alzheimer's disease are independent of caspase cleavage of the amyloid precursor protein. J Neurosci 2010;30:372–381. [PubMed: 20053918]

Haughey NJ, Nath A, Chan SL, Borchard AC, Rao MS, Mattson MP. Disruption of neurogenesis by amyloid beta-peptide, and perturbed neural progenitor cell homeostasis, in models of Alzheimer's disease. J Neurochem 2002;83:1509–1524. [PubMed: 12472904]

He J, Yamada K, Nabeshima T. A role of Fos expression in the CA3 region of the hippocampus in spatial memory formation in rats. Neuropsychopharmacology 2002;26:259–268. [PubMed: 11790521]

Hsia A, Masliah E, McConlogue L, Yu G, Tatsuno G, Hu K, Kholodenko D, Malenka RC, Nicoll RA, Mucke L. Plaque-independent disruption of neural circuits in Alzheimer's disease mouse models. Proc Natl Acad Sci USA 1999;96:3228–3233. [PubMed: 10077666]

Hsiao K, Chapman P, Nilsen S, Eckman C, Harigaya Y, Younkin S, Yang FS, Cole G. Correlative memory deficits, Aβ elevation, and amyloid plaques in transgenic mice. Science 1996;274:99–102. [PubMed: 8810256]

Insausti R, Herrero MT, Witter MP. Entorhinal cortex of the rat: cytoarchitectonic subdivisions and the origin and distribution of cortical efferents. Hippocampus 1997;7:146–183. [PubMed: 9136047]

Jankowsky JL, Slunt HH, Gonzales V, Savonenko AV, Wen JC, Jenkins NA, Copeland NG, Younkin LH, Lester HA, Younkin SG, Borchelt DR. Persistent amyloidosis following suppression of Aβ production in a transgenic model of Alzheimer disease. PLoS Med 2005;2:e355(1318)–e1355(1333). [PubMed: 16279840]

Johnson-Wood K, Lee M, Motter R, Hu K, Gordon G, Barbour R, Khan K, Gordon M, Tan H, Games D, Lieberburg I, Schenk D, Seubert P, McConlogue L. Amyloid precursor protein processing and $A\beta_{42}$ deposition in a transgenic mouse model of Alzheimer disease. Proc Natl Acad Sci USA 1997;94:1550–1555. [PubMed: 9037091]

Jones BF, Witter MP. Cingulate cortex projections to the parahippocampal region and hippocampal formation in the rat. Hippocampus 2007;17:957–976. [PubMed: 17598159]

Kamenetz F, Tomita T, Hsieh H, Seabrook G, Borchelt D, Iwatsubo T, Sisodia S, Malinow R. APP processing and synaptic function. Neuron 2003;37:925–937. [PubMed: 12670422]

Kirkby DL, Higgins GA. Characterization of perforant path lesions in rodent models of memory and attention. Eur J Neurosci 1998;10:823–838. [PubMed: 9753151]

Kjelstrup KG, Tuvnes FA, Steffenach HA, Murison R, Moser EI, Moser MB. Reduced fear expression after lesions of the ventral hippocampus. Proc Natl Acad Sci USA 2002;99:10825–10830. [PubMed: 12149439]

Kobayashi DT, Chen KS. Behavioral phenotypes of amyloid-based genetically modified mouse models of Alzheimer's Disease. Genes Brain and Behav 2005;4:173–196.

Lanz TA, Hosley JD, Adams WJ, Merchant KM. Studies of Abeta pharmacodynamics in the brain, cerebrospinal fluid, and plasma in young (plaque-free) Tg2576 mice using the gamma-secretase inhibitor N2-[(2S)-2-(3,5-difluorophenyl)-2-hydroxyethanoyl]-N1-[(7S)-5-methyl-6-oxo -6,7-dihydro-5H-dibenzo[b,d]azepin-7-yl]-L-alaninamide (LY-411575). J Pharmacol Exp Ther 2004;309:49–55. [PubMed: 14718585]

Lazarov O, Lee M, Peterson DA, Sisodia SS. Evidence that synaptically released beta-amyloid accumulates as extracellular deposits in the hippocampus of transgenic mice. J Neurosci 2002;22:9785–9793. [PubMed: 12427834]

Liang WS, Dunckley T, Beach TG, Grover A, Mastroeni D, Ramsey K, Caselli RJ, Kukull WA, McKeel D, Morris JC, Hulette CM, Schmechel D, Reiman EM, Rogers J, Stephan DA. Altered neuronal gene expression in brain regions differentially affected by Alzheimer's disease: a reference data set. Physiol Genomics 2008;33:240–256. [PubMed: 18270320]

Liang WS, Dunckley T, Beach TG, Grover A, Mastroeni D, Walker DG, Caselli RJ, Kukull WA, McKeel D, Morris JC, Hulette C, Schmechel D, Alexander GE, Reiman EM, Rogers J, Stephan DA. Gene expression profiles in anatomically and functionally distinct regions of the normal aged human brain. Physiol Genomics 2007;28:311–322. [PubMed: 17077275]

Lopez-Toledano MA, Shelanski ML. Increased neurogenesis in young transgenic mice overexpressing human APP(Sw, Ind). J Alzheimers Dis 2007;12:229–240. [PubMed: 18057556]

Masdeu JC, Zubieta JL, Arbizu J. Neuroimaging as a marker of the onset and progression of Alzheimer's disease. J Neurol Sci 2005;236:55–64. [PubMed: 15961110]

McDonald AJ. Cortical pathways to the mammalian amygdala. Prog Neurobiol 1998;55:257–332. [PubMed: 9643556]

Meilandt WJ, Yu G-Q, Chin J, Roberson ED, Palop JJ, Wu T, Scearce-Levie K, Mucke L. Enkephalin elevations contribute to neuronal and behavioral impairments in a transgenic mouse model of Alzheimer's disease. J Neurosci 2008;28:5007–5017. [PubMed: 18463254]

Meilandt WJ, Cisse M, Ho K, Wu T, Esposito LA, Scearce-Levie K, Cheng IH, Yu GQ, Mucke L. Neprilysin overexpression inhibits plaque formation but fails to reduce pathogenic Abeta oligomers and associated cognitive deficits in human amyloid precursor protein transgenic mice. J Neurosci 2009;29:1977–1986. [PubMed: 19228952]

Meyer-Luehmann M, Coomaraswamy J, Bolmont T, Kaeser S, Schaefer C, Kilger E, Neuenschwander A, Abramowski D, Frey P, Jaton AL, Vigouret JM, Paganetti P, Walsh DM, Mathews PM, Ghiso J, Staufenbiel M, Walker LC, Jucker M. Exogenous induction of cerebral beta-amyloidogenesis is governed by agent and host. Science 2006;313:1781–1784. [PubMed: 16990547]

Minkeviciene R, Rheims S, Dobszay MB, Zilberter M, Hartikainen J, Fulop L, Penke B, Zilberter Y, Harkany T, Pitkanen A, Tanila H. Amyloid beta-induced neuronal hyperexcitability triggers progressive epilepsy. J Neurosci 2009;29:3453–3462. [PubMed: 19295151]

Molinari S, Battini R, Ferrari S, Pozzi L, Killcross AS, Robbins TW, Jouvenceau A, Billard J-M, Dutar P, Lamour Y, Baker WA, Cox H, Emson PC. Deficits in memory and hippocampal long-term potentiation in mice with reduced calbindin D_{28K} expression. Proc Natl Acad Sci USA 1996;93:8028–8033. [PubMed: 8755597]

Mucke L, Abraham CR, Ruppe MD, Rockenstein EM, Toggas SM, Alford M, Masliah E. Protection against HIV-1 gp120-induced brain damage by neuronal expression of human amyloid precursor protein. J Exp Med 1995;181:1551–1556. [PubMed: 7699335]

Mucke L, Masliah E, Yu G-Q, Mallory M, Rockenstein EM, Tatsuno G, Hu K, Kholodenko D, Johnson-Wood K, McConlogue L. High-level neuronal expression of $A\beta_{1–42}$ in wild-type human amyloid protein precursor transgenic mice: Synaptotoxicity without plaque formation. J Neurosci 2000;20:4050–4058. [PubMed: 10818140]

Nagahara AH, Merrill DA, Coppola G, Tsukada S, Schroeder BE, Shaked GM, Wang L, Blesch A, Kim A, Conner JM, Rockenstein E, Chao MV, Koo EH, Geschwind D, Masliah E, Chiba AA, Tuszynski MH. Neuroprotective effects of brain-derived neurotrophic factor in rodent and primate models of Alzheimer's disease. Nat Med 2009;15:331–337. [PubMed: 19198615]

Nikolaev A, McLaughlin T, O'Leary DD, Tessier-Lavigne M. APP binds DR6 to trigger axon pruning and neuron death via distinct caspases. Nature 2009;457:981–989. [PubMed: 19225519]

Ognibene E, Middei S, Daniele S, Adriani W, Ghirardi O, Caprioli A, Laviola G. Aspects of spatial memory and behavioral disinhibition in Tg2576 transgenic mice as a model of Alzheimer's disease. Behav Brain Res 2005;156:225–232. [PubMed: 15582108]

Palop JJ, Mucke L. Synaptic Depression and Aberrant Excitatory Network Activity in Alzheimer's Disease: Two Faces of the Same Coin? Neuromolecular Med 2009:48–55. [PubMed: 19838821]

Palop JJ, Mucke L. Amyloid-beta-induced neuronal dysfunction in Alzheimer's disease: from synapses toward neural networks. Nat Neurosci 2010;13:812–818. [PubMed: 20581818]

Palop JJ, Chin J, Mucke L. A network dysfunction perspective on neurodegenerative diseases. Nature 2006;443:768–773. [PubMed: 17051202]

Palop JJ, Chin J, Bien-Ly N, Massaro C, Yeung BZ, Yu G-Q, Mucke L. Vulnerability of dentate granule cells to disruption of Arc expression in human amyloid precursor protein transgenic mice. J Neurosci 2005;25:9686–9693. [PubMed: 16237173]

Palop JJ, Jones B, Kekonius L, Chin J, Yu G-Q, Raber J, Masliah E, Mucke L. Neuronal depletion of calcium-dependent proteins in the dentate gyrus is tightly linked to Alzheimer's disease-related cognitive deficits. Proc Natl Acad Sci USA 2003;100:9572–9577. [PubMed: 12881482]

Palop JJ, Chin J, Roberson ED, Wang J, Thwin MT, Bien-Ly N, Yoo J, Ho KO, Yu G-Q, Kreitzer A, Finkbeiner S, Noebels JL, Mucke L. Aberrant excitatory neuronal activity and compensatory remodeling of inhibitory hippocampal circuits in mouse models of Alzheimer's disease. Neuron 2007;55:697–711. [PubMed: 17785178]

Ramirez JJ, Campbell D, Poulton W, Barton C, Swails J, Geghman K, Courchesne SL, Wentworth S. Bilateral entorhinal cortex lesions impair acquisition of delayed spatial alternation in rats. Neurobiol Learn Mem 2007;87:264–268. [PubMed: 17049284]

Remondes M, Schuman EM. Role for a cortical input to hippocampal area CA1 in the consolidation of a long-term memory. Nature 2004;431:699–703. [PubMed: 15470431]

Roberson ED, Scearce-Levie K, Palop JJ, Yan F, Cheng IH, Wu T, Gerstein H, Yu G-Q, Mucke L. Reducing endogenous tau ameliorates amyloid β-induced deficits in an Alzheimer's disease mouse model. Science 2007;316:750–754. [PubMed: 17478722]

Roberts GW, Nash M, Ince PG, Royston MC, Gentleman SM. On the origin of Alzheimer's disease: A hypothesis. NeuroReport 1993;4:7–9. [PubMed: 8453040]

Scheff SW, Price DA. Synaptic pathology in Alzheimer's disease: A review of ultrastructural studies. Neurobiol Aging 2003;24:1029–1046. [PubMed: 14643375]

Seeley WW, Crawford RK, Zhou J, Miller BL, Greicius MD. Neurodegenerative diseases target large-scale human brain networks. Neuron 2009;62:42–52. [PubMed: 19376066]

Selkoe DJ. Soluble oligomers of the amyloid beta-protein impair synaptic plasticity and behavior. Behav Brain Res 2008;192:106–113. [PubMed: 18359102]

Shankar GM, Li S, Mehta TH, Garcia-Munoz A, Shepardson NE, Smith I, Brett FM, Farrell MA, Rowan MJ, Lemere CA, Regan CM, Walsh DM, Sabatini BL, Selkoe DJ. Amyloid-beta protein dimers isolated directly from Alzheimer's brains impair synaptic plasticity and memory. Nat Med 2008;14:837–842. [PubMed: 18568035]

Sheng JG, Price DL, Koliatsos VE. Disruption of corticocortical connections ameliorates amyloid burden in terminal fields in a transgenic model of Abeta amyloidosis. J Neurosci 2002;22:9794–9799. [PubMed: 12427835]

Spencer B, Rockenstein E, Crews L, Marr R, Masliah E. Novel strategies for Alzheimer's disease treatment. Expert Opin Biol Ther 2007;7:1853–1867. [PubMed: 18034651]

Sperling RA, Laviolette PS, O'Keefe K, O'Brien J, Rentz DM, Pihlajamaki M, Marshall G, Hyman BT, Selkoe DJ, Hedden T, Buckner RL, Becker JA, Johnson KA. Amyloid deposition is associated with impaired default network function in older persons without dementia. Neuron 2009;63:178–188. [PubMed: 19640477]

Squire LR, Stark CE, Clark RE. The medial temporal lobe. Annu Rev Neurosci 2004;27:279–306. [PubMed: 15217334]

Steffenach HA, Witter M, Moser MB, Moser EI. Spatial memory in the rat requires the dorsolateral band of the entorhinal cortex. Neuron 2005;45:301–313. [PubMed: 15664181]

Sun B, Halabisky B, Zhou Y, Palop JJ, Yu GQ, Mucke L, Gan L. Imbalance between GABAergic and glutamatergic transmissions impairs adult neurogenesis in an animal model of Alzheimer's disease. Cell Stem Cell 2009;5:624–633. [PubMed: 19951690]

Sun B, Zhou Y, Halabisky B, Lo I, Cho SH, Mueller-Steiner S, Devidze N, Wang X, Grubb A, Gan L. Cystatin C-cathepsin B axis regulates amyloid beta levels and associated neuronal deficits in an animal model of Alzheimer's disease. Neuron 2008;60:247–257. [PubMed: 18957217]

Sze CI, Troncoso JC, Kawas C, Mouton P, Price DL, Martin LJ. Loss of the presynaptic vesicle protein synaptophysin in hippocampus correlates with cognitive decline in Alzheimer disease. J Neuropathol Exp Neurol 1997;56:933–944. [PubMed: 9258263]

Tanzi R, Bertram L. Twenty years of the Alzheimer's disease amyloid hypothesis: A genetic perspective. Cell 2005;120:545–555. [PubMed: 15734686]

Tanzi RE. The synaptic Ab hypothesis of Alzheimer disease. Nat Neurosci 2005;8:977–979. [PubMed: 16047022]

Terry RD, Masliah E, Salmon DP, Butters N, DeTeresa R, Hill R, Hansen LA, Katzman R. Physical basis of cognitive alterations in Alzheimer's disease: Synapse loss is the major correlate of cognitive impairment. Ann Neurol 1991;30:572–580. [PubMed: 1789684]

Tomiyama T, Matsuyama S, Iso H, Umeda T, Takuma H, Ohnishi K, Ishibashi K, Teraoka R, Sakama N, Yamashita T, Nishitsuji K, Ito K, Shimada H, Lambert MP, Klein WL, Mori H. A mouse model of amyloid beta oligomers: their contribution to synaptic alteration, abnormal tau phosphorylation, glial activation, and neuronal loss in vivo. J Neurosci 2010;30:4845–4856. [PubMed: 20371804]

Tuszynski MH, Thal L, Pay M, Salmon DP, UHS, Bakay R, Patel P, Blesch A, Vahlsing HL, Ho G, Tong G, Potkin SG, Fallon J, Hansen L, Mufson EJ, Kordower JH, Gall C, Conner J. A phase 1 clinical trial of nerve growth factor gene therapy for Alzheimer disease. Nat Med 2005;11:551–555. [PubMed: 15852017]

van Groen T, Wyss JM. Connections of the retrosplenial granular a cortex in the rat. J Comp Neurol 1990;300:593–606. [PubMed: 2273095]

van Groen T, Wyss JM. Connections of the retrosplenial dysgranular cortex in the rat. J Comp Neurol 1992;315:200–216. [PubMed: 1545009]

Van Groen T, Wyss JM. Connections of the retrosplenial granular b cortex in the rat. J Comp Neurol 2003;463:249–263. [PubMed: 12820159]

van Groen T, Miettinen P, Kadish I. The entorhinal cortex of the mouse: Organization of the projection to the hippocampal formation. Hippocampus 2003;13:133–149. [PubMed: 12625464]

van Strien NM, Cappaert NL, Witter MP. The anatomy of memory: an interactive overview of the parahippocampal-hippocampal network. Nat Rev Neurosci 2009;10:272–282. [PubMed: 19300446]

Vann SD, Aggleton JP, Maguire EA. What does the retrosplenial cortex do? Nat Rev Neurosci 2009;10:792–802. [PubMed: 19812579]

Verret L, Trouche S, Zerwas M, Rampon C. Hippocampal neurogenesis during normal and pathological aging. Psychoneuroendocrinology 2007;32(Suppl 1):S26–S30. [PubMed: 17629417]

Walsh DM, Selkoe DJ. Deciphering the molecular basis of memory failure in Alzheimer's disease. Neuron 2004;44:181–193. [PubMed: 15450169]

Wei W, Nguyen LN, Kessels HW, Hagiwara H, Sisodia S, Malinow R. Amyloid beta from axons and dendrites reduces local spine number and plasticity. Nat Neurosci 2010;13:190–196. [PubMed: 20037574]

Weidemann A, Paliga K, Dürrwang U, Reinhard FBM, Schuckert O, Evin G, Masters CL. Proteolytic processing of the Alzheimer's disease amyloid precursor protein within its cytoplasmic domain by caspase-like proteases. J Biol Chem 1999;274:5823–5829. [PubMed: 10026204]

Wu W, Small SA. Imaging the earliest stages of Alzheimer's disease. Curr Alzheimer Res 2006;3:529–539. [PubMed: 17168652]

Wyss JM, Van Groen T. Connections between the retrosplenial cortex and the hippocampal formation in the rat: a review. Hippocampus 1992;2:1–11. [PubMed: 1308170]

Yasuda M, Mayford MR. CaMKII activation in the entorhinal cortex disrupts previously encoded spatial memory. Neuron 2006;50:309–318. [PubMed: 16630840]

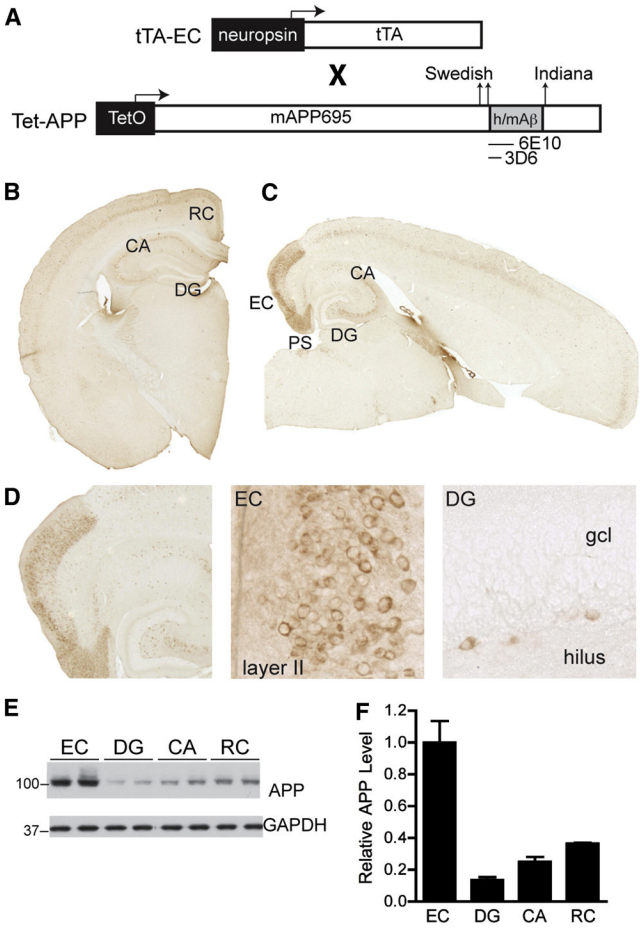

Figure 1.

Restricted cortical expression of mutant APP in EC-APP mice. (A) Transgenes used to generate the tTA-EC and tet-APP mouse lines. When crossed, mice carrying both transgenes expressed transgenic APP primarily in the EC. Representative images of coronal (B) and horizontal (C) brain sections from EC-APP mice stained for the transgene-derived chimeric human/mouse APP (h/mAPP) with anti-human Aβ antibody 6E10. Prominent APP expression was observed primarily in the medial EC and in the pre- and para-subiculum (PS). Hippocampal APP labeling in EC-APP mice was faint in scattered cells of the CA regions. (D) Higher magnification images of the EC and DG in an EC-APP mouse showing neuronal expression of APP predominantly in superficial layers of the EC. No transgene expression was observed in the granular cell layer (gcl) of the DG; a few scattered APP-positive cells were seen in the hilus. (E,F) Relative APP levels in different brain regions of EC-APP mice were determined by western blotting (E) and signals were quantified by densitometry (F). GAPDH served as a loading control. The EC had the highest APP levels, followed by the RC, whose APP levels were less than 40% of those in the EC. Values are mean ± SEM.

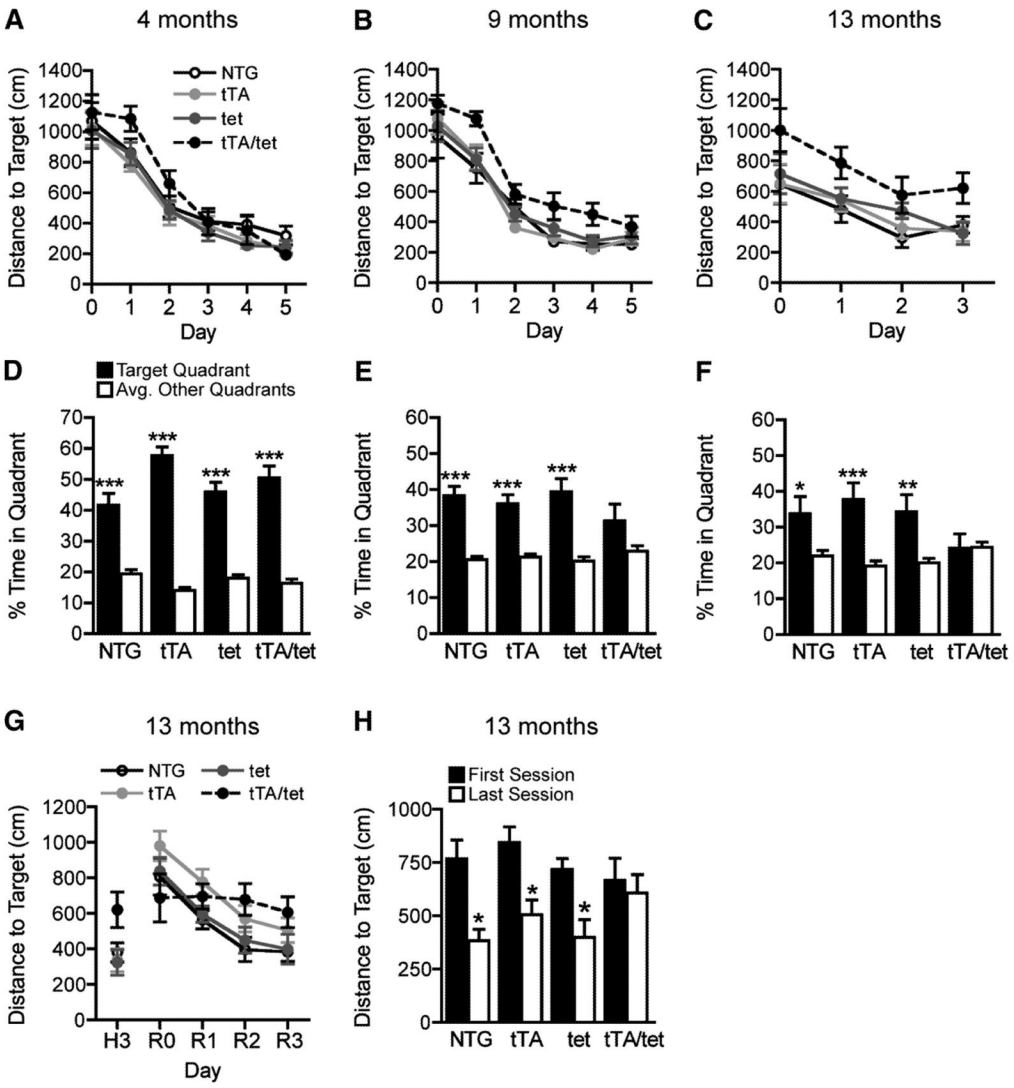

Figure 2.

EC-APP mice have age-dependent deficits in spatial learning and memory. At 4 (A), 9 (B) and 13 (C) months of age, mice of the four genotypes were trained for 3–5 days to locate a hidden platform in the MWM. The time (not shown) and path length (distance) to reach the hidden platform were recorded. By 9 months, EC-APP (tTA/tet) mice showed impaired learning relative to the other groups ($p<0.001$ for genotype by repeated-measures ANOVA). Their learning deficits persisted at 13 months ($p<0.01$ for genotype by repeated-measures ANOVA). Latencies to reach the platform revealed similar learning deficits in EC-APP mice, and swim speeds did not differ among the groups (data not shown). (D–F) For each age group, probe trials (platform removed) were conducted 24h after the last training session. At 4 months, all groups showed a clear preference for the target quadrant, suggesting normal learning and memory retention. At 9 months, only EC-APP mice failed to spend significantly more time in the target quadrant than in the other quadrants. At 13 months, EC-APP mice spent comparable proportions of time in target and non-target quadrants, whereas the other groups still favored the target quadrant. (G–H) EC-APP mice have deficits in a spatial reversal-learning task. After the probe trial in (F), the location of the platform was changed and mice were trained for another 3 days to locate the new

platform location (reversal phase). (G) In contrast to the control groups, EC-APP mice failed to improve their performance during the learning phase of this reversal task ($p<0.0005$ for effect of training day by repeated-measures ANOVA in the control groups only). (H) Distances to the new target location were shorter in the last than the first training sessions in the control groups, but not in EC-APP mice. *$p<0.05$, **$p<0.005$, ***$p<0.0005$ vs. the average percent time spent in nontarget quadrants by *t* test (D–F) or vs. the first session by *t* test (H). n=10–13 mice/group. Values are mean ± SEM.

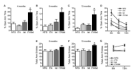

Figure 3.

EC-APP mice show abnormal phenotypes in the elevated plus maze and Y-maze. (A–C) Percent time spent in the open arms of an elevated plus maze was recorded over a 5 min period. At all ages, EC-APP (tTA/tet) mice spent more time in the open arms than the three control groups. *p<0.05, vs. all other groups by ANOVA and Tukey test. (D) All groups spent less and less time in the open arms during subsequent tests, possibly because of aging, habituation to the elevated plus maze, or both. p<0.0001, for effects of genotype and age by 2-way ANOVA. (E–G) EC-APP mice are hyperactive in the Y-maze. Total arm entries were monitored over a 6 min period at 9 (E) and 13 (F) months. Compared with the control groups, EC-APP (tTA/tet) mice showed a trend toward increased activity at 9 months and clear hyperactivity at 13 months. *p<0.05 vs. all other groups by ANOVA and Newman-Keuls post hoc test. (G) None of the groups showed habituation in Y-maze activity during the second exposure. p<0.05 for genotype only by 2-way ANOVA. n=10–13 mice/group. Values are mean ± SEM.

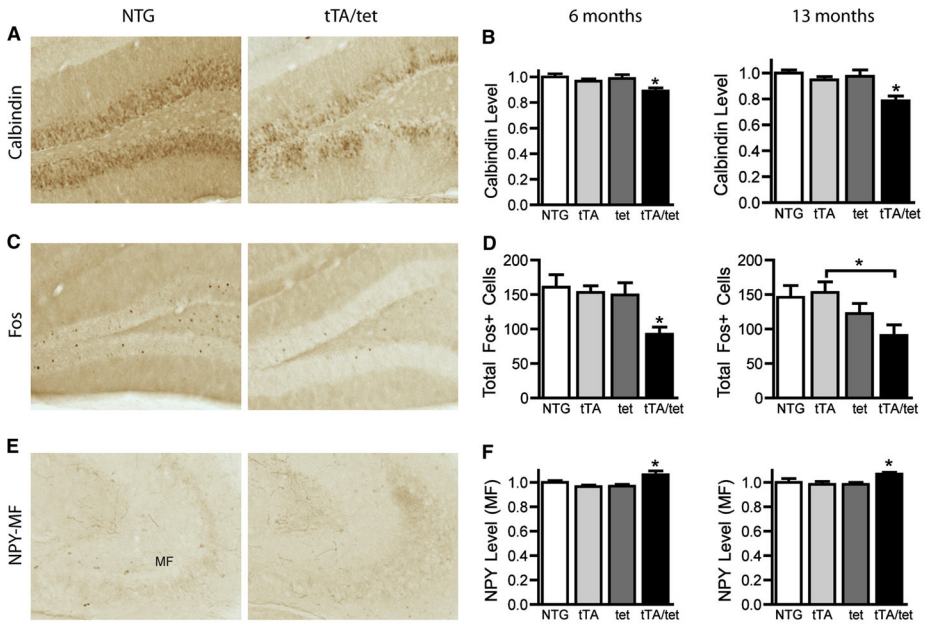

Figure 4.

EC-APP mice have abnormalities in synaptic activity-related proteins in the DG. Brain sections from mice of the four genotypes were immunostained for calbindin, Fos, or NPY. Immunoreactivity for calbindin in the molecular layer and for NPY in the mossy fiber (MF) pathway was determined by densitometry; Fos-positive neurons were counted in the granular cell layer. Representative coronal sections of the DG from 6-month-old NTG and EC-APP (tTA/tet) mice (A,C,E) and quantitative results from 6- and 13-month-old mice (B,D,F). ANOVA revealed a significant effect of genotype on all measures. *$p<0.05$ vs. all other groups, or as indicated by brackets with Newman-Keuls post-hoc test. n=14–15 mice/group (6 months) or n=6–9 mice/group (13 months). Values are mean ± SEM.

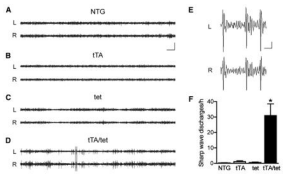

Figure 5.

Epileptiform activity in parietal cortex of EC-APP mice. Bilateral EEG recordings were performed in 4–5-month-old mice of all four genotypes for 24 h. (A–C) Representative traces from control groups show normal EEG activity with no or very infrequent sharp wave discharges (SWDs). (D) In contrast, EC-APP (tTA/tet) mice displayed frequent SWDs. (E) The gray area in (D) was magnified to reveal the waveforms of the spike discharges in EC-APP mice. (F) Quantification of total SWDs per hour revealed a significantly greater frequency of SWDs in EC-APP mice than in all other groups. $p<0.0005$ for genotype by ANOVA and $^{*}p<0.05$ vs. all other groups by Tukey post-hoc test. n=4–7 mice/group. L, left parietal cortex; R, right parietal cortex. Values are mean ± SEM. Scale bars: A, 10 s and 500 μV; E, 0.5 s and 100 μV.

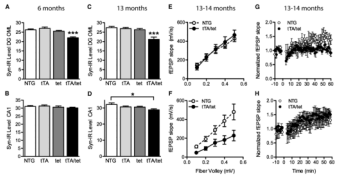

Figure 6.

Synaptic deficits in EC-APP mice. (A–D) Percent area of sections occupied by synaptophysin-immunoreactive structures in the outer molecular layer of the DG and stratum radiatum of CA1 in mice at 6 (A,B) and 13 (C,D) months of age. (A,C) At both ages, synaptophysin levels were lower in the DG of EC-APP (tTA/tet) mice than in all control groups. (B,D) Genotype affected synaptophysin levels in CA1 at 13, but not 6, months. n=6–9 mice/group. *$p<0.05$, ***$p<0.0005$ vs. all other groups, or as indicated by the bracket (Tukey post-hoc test). Values are mean ± SEM. (E–H) Electrophysiological recordings were obtained in acute hippocampal slices from 13–14-month-old EC-APP and NTG mice. The input-output relationship in EC-APP mice was normal, compared with NTG mice, at the perforant path-granule cell synapse in the DG (E; n=6–7 slices from 3 mice/genotype), but impaired at the Schaffer collateral-CA1 synapse (F; $p<0.05$ by 2-way repeated-measures ANOVA, n=9–10 slices from 3–5 mice/genotype). LTP was impaired at the perforant path-granule cell synapse in the DG of EC-APP mice relative to controls (G; $p<0.05$ by repeated-measures ANOVA from minutes 50–60, n=3–4 slices from 3 mice/genotype), but not at the Schaffer collateral-CA1 synapse (H; n=3–4 slices from 2–3 mice/genotype).

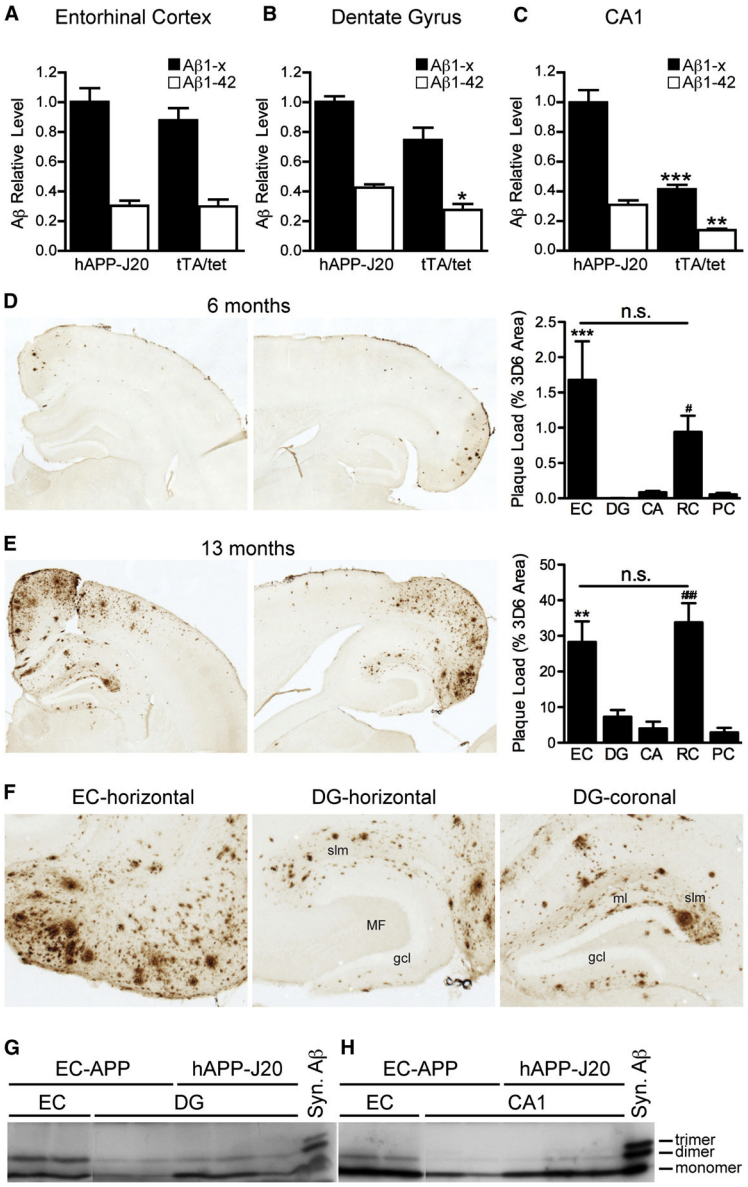

Figure 7.

Aβ levels and plaque distribution in interconnected brain regions of young and older EC-APP mice. Soluble levels of Aβ1-x and Aβ1–42 were measured before plaque formation in the EC (A), DG (B), and CA1 (C) by ELISA in 3-month-old EC-APP (tTA/tet) mice and age-matched hAPP-J20 mice. Levels of Aβ1-x and Aβ1–42 in the EC and Aβ1-x in the DG were comparable in EC-APP mice and hAPP-J20 mice. Levels of Aβ1-x and Aβ1–42 in CA1 and of Aβ1–42 in the DG were lower in EC-APP mice than in hAPP-J20 mice, which have widespread expression of hAPP. n=3–4 mice/genotype. *p<0.05, **p<0.005, ***p<0.0005 vs. hAPP-J20 by *t* test. (D–F) Immunostaining for Aβ with the 3D6 antibody revealed an age-dependent increase in Aβ deposition in the EC, DG, CA, RC, and PC of EC-APP mice. (D,E) Representative coronal (left) and horizontal (middle) brain sections for each age. Percent area covered by 3D6-immunoreactive Aβ deposits was quantified to determine “plaque loads.” Horizontal sections were used for EC and coronal sections for DG, CA, RC, and PC. Numbers of mice analyzed: at 6 months, n=15 (coronal; DG, CA, RC,

PC) and 9 (horizontal; EC); at 13 months, n=7 (coronal) and 4 (horizontal). n.s. not significant, **p<0.005, ***p<0.0005 EC vs. DG, CA, and PC; $^{\#}$p<0.05, $^{\#\#\#}$p<0.0005 RC vs DG, CA, and PC by ANOVA and Tukey post-hoc test. Values are mean ± SEM. (F) Higher-magnification images from 13-month-old mice showing plaque deposition throughout the EC (left). In the DG (middle and right), plaques were localized predominantly in the terminal fields of perforant pathway axons from the EC: stratum lacunosum moleculare (slm) and ml. (G, H) Small oligomeric forms of Aβ were detected by immunoprecipitation/ western blotting in different brain regions of 13-month-old EC-APP and hAPP-J20 mice. Aβ dimers were present in all brain regions analyzed; the highest levels were in the EC of EC-APP mice. Syn., synthetic.

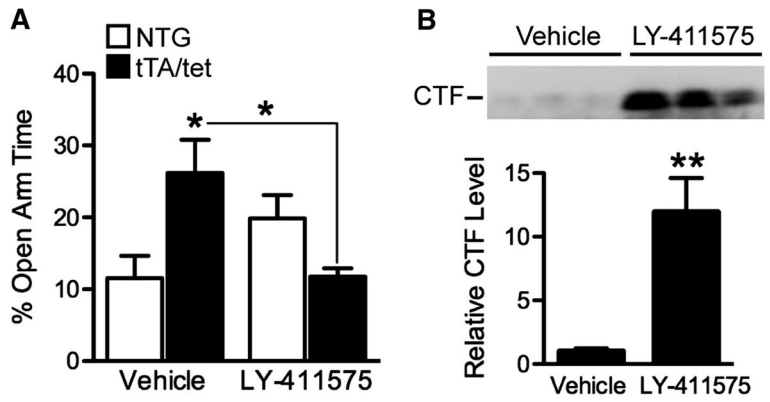

Figure 8.

Inhibiting γ-secretase cleavage to reduce Aβ production normalizes EPM behavior in 4-month-old EC-APP mice. Mice were injected once a day with LY-411575 (3mg/kg) or vehicle on two consecutive days and tested in the EPM 6–8 h after the second injection. (A) Vehicle-treated EC-APP (tTA/tet) mice spent more time in the open arms of the EPM than vehicle-treated NTG mice. LY-411575 treatment significantly reduced the amount of time EC-APP mice spent in the open arms to the levels in vehicle-treated NTG controls. n=5–7 mice/group. $p<0.005$ for the interaction effect between genotype and treatment by 2-way ANOVA, *$p<0.05$ vs. NTG+vehicle or as indicated by bracket (one-way ANOVA followed by Tukey post-hoc test). (B) APP CTFs in the EC of EC-APP mice were measured by Western blotting and quantified by densitometry. Inhibition of γ-secretase cleavage increased CTF levels in EC-APP mice. n=5–7 mice/group. **$p<0.005$ vs. vehicle by *t* test. Values are mean ± SEM.